

Two-step magnetization in a spin-chain system on the triangular lattice: Wang-Landau simulation

M. H. Qin and K. F. Wang

Laboratory of Solid State Microstructures, Nanjing University, Nanjing 210093, China

J. M. Liu*

*Laboratory of Solid State Microstructures, Nanjing University, Nanjing 210093, China;**School of Physics, South China Normal University, Guangzhou 510006, China;**and International Center for Materials Physics, Chinese Academy of Science, Shenyang 110016, China*

(Received 7 March 2009; published 13 May 2009)

The Wang-Landau algorithm is used to study the thermodynamic and magnetic properties of triangular spin-chain system based on two-dimensional Ising model in order to understand the magnetic-order dynamics in $\text{Ca}_3\text{Co}_2\text{O}_6$ compound. The calculated results demonstrate that the equilibrium state of the rigid spins produces the two-step magnetization curve at low temperature even when the random-exchange term is considered. This work indicates that the four-step magnetization behavior observed experimentally must be due to the nonequilibrium magnetization.

DOI: [10.1103/PhysRevB.79.172405](https://doi.org/10.1103/PhysRevB.79.172405)

PACS number(s): 75.40.Mg, 02.70.Uu, 05.50.+q

During the past few years, spin-chain system $\text{Ca}_3\text{Co}_2\text{O}_6$ has drawn considerable attention from both experimental and theoretical points of view due to their unique magnetic behaviors.¹⁻¹⁷ As revealed experimentally, $\text{Ca}_3\text{Co}_2\text{O}_6$ has a rhombohedral structure composed of Co_2O_6 chains running along the c axis of the corresponding hexagonal cell. The Ca ions are situated between them and are not involved in magnetic interactions.¹ These chains are built by alternating, face-sharing CoO_6 trigonal prisms and CoO_6 octahedral. Each chain is surrounded by six equally spaced chains, forming a triangular lattice on the ab plane that is perpendicular to the chains along the c axis.

The most intriguing feature for such a spin-chain system is a steplike magnetization (M) as a function of external magnetic field (B) applied along the chains. Experimentally, two steps are observed in the temperature (T) range of 10–25 K. Close to $B=0$, M reaches the first plateau at $M=M_0/3$ (where M_0 is the saturated magnetization). Then the plateau stretches up to $B=3.6$ T where M springs up to M_0 . Experimentally, when $T<10$ K, the first step at $M_0/3$ splits into three equidistant steps at a slow magnetic-field sweep rate, thus constituting a four-step magnetization pattern. The origin of such four-steplike magnetization behavior has been extensively studied most recently, and it is still a matter of debate.⁷⁻⁹

For $\text{Ca}_3\text{Co}_2\text{O}_6$, because the intrachain-ferromagnetic (FM) interaction is much stronger than the interchain-antiferromagnetic (AFM) coupling, the chains can be assumed to be in two ordered states (spin-up or spin-down) at low T . Based on this basic assumption, Kudasov developed a two-dimensional (2D) Ising model to investigate the steplike magnetization by an analytical method regarding a spin chain as a large rigid spin and assuming a quench at $T=0$.⁹ By this theory at the fourth approximations, four equidistant steps can be produced in accordance with experimental curves. Similar model was proposed and employed for exploring the static magnetization behavior of $\text{Ca}_3\text{Co}_2\text{O}_6$ using Monte Carlo simulation,^{15,16} and the four-step behavior, consistent with experimental observation, was confirmed when a random-exchange term was taken into account.

Nevertheless, recent experiments seemed to question this four-step magnetization once more. It was observed that the number of the steps in the magnetization curve strongly depends on the sweep rate of magnetic field B . As the sweep rate is decreased, some of the magnetization steps disappear. This phenomenon shows that the four-step magnetization curve may be due to the nonequilibrium magnetization dynamics. Most recently, Kudasov *et al.*¹¹ performed the simulation of the nonequilibrium evolution by means of a Glauber-type form of the spin-flip probability and investigated the dependence of the magnetization curves on the magnetic-field sweep rate in good agreement with the experimental data. In addition, the influence of metastable states on the magnetic behavior in $\text{Ca}_3\text{Co}_2\text{O}_6$ compound has been studied in detail using the same model.¹⁴ As the relaxation time increases, the first three plateaus observed at low T tend to merge into one step, likely generating eventually a two-step pattern. These works seem to indicate that the spin-chain system of triangular lattice under B at low T is easily trapped into metastable states from equilibrium and probably the equilibrium state of the magnetization dynamics is not of four-step pattern.

Therefore, it is still an unsolved issue to demonstrate this equilibrium pattern in order to understand the magnetic behavior of the system. However, conventional Metropolis algorithm of Monte Carlo simulation based on local spin flip often fails to relax into the equilibrium state because the model we studied here contains the frustration in the exchange interaction due to the triangular lattice geometry. To overcome this difficulty, one can appeal to the Wang-Landau (WL) algorithm which enables the system to avoid trapping to a metastable state because this algorithm is very powerful to reach the ground state (equilibrium state). Since it was proposed in 2001,^{18,19} the WL algorithm has been successfully applied to various problems, such as complex spin models,²⁰⁻²² quantum systems,^{23,24} fluids,^{25,26} and proteins.^{27,28} However, as far as we know, there has been no work on the magnetic properties of $\text{Ca}_3\text{Co}_2\text{O}_6$ approached by the WL algorithm in any quantitative sense. In this article, we shall use the standard WL algorithm to calculate the ther-

TABLE I. Parameters chosen for the simulation.

Parameter	Value	Parameter	Value
$k_B(J/K)$	1.3807×10^{-23}	$J(J)$	3.592×10^{-25}
$\mu_B(J/T)$	9.274×10^{-24}	S	32
g	2		

modynamic and magnetic properties of $\text{Ca}_3\text{Co}_2\text{O}_6$ in order to understand the complex magnetic order at the equilibrium state.

Based on the rigid-chain model,⁹ the three-dimensional issue of $\text{Ca}_3\text{Co}_2\text{O}_6$ is reduced to the 2D AFM triangular Ising model²⁹

$$H = J \sum_{[m,n]} S_m S_n - B \mu_B g \sum_m S_m, \quad (1)$$

where $J > 0$ is the AFM-interchain coupling, S_m is the effective spin moment of a spin chain at the site m with the value S , B is an external magnetic field applied along the direction of up-spin chains ($+c$ axis), g is the Lande factor, and μ_B is the Bohr magneton; $[m,n]$ denotes the summation over all the nearest-neighbor pairs.

For investigating the magnetic properties of a system with the WL algorithm, one has to calculate the density of state (DOS) $g(E, M)$ in energy and magnetization space where E denotes the energy of a given spin configuration of the Hamiltonian without external field. Following the pathbreaking work of Wang and Landau,^{18,19} we choose the simulation procedure stated in Refs. 18 and 19.

At the very beginning, we set all entries to the DOS $g(E, M) = 1$ and a histogram $RH(E, M) = 0$ for all possible (E, M) states. Then we begin our random walk in the energy and magnetization space by flipping spins randomly. The transition probability from state (E_1, M_1) to state (E_2, M_2) is

$$p(E_1, M_1 \rightarrow E_2, M_2) = \min \left[\frac{g(E_2, M_2)}{g(E_1, M_1)}, 1 \right], \quad (2)$$

where states (E_1, M_1) and (E_2, M_2) , respectively, denote energies and magnetizations before and after a spin is flipped. Each time a new state (E_i, M_i) is visited, we modify the existing DOS by a modification factor f_0 ; i.e., $g(E_i, M_i) = g(E_i, M_i) f_0$. In this Brief Report an initial modification factor of $f_0 = \exp(1)$, which allows us to reach all possible energy levels quickly, is used. If the random walk rejects a possible move and stays at the same state (E, M) , we also modify the existing DOS by the same modification factor. Each time, the histogram $RH(E_i, M_i)$ (the number of visits) in the energy and magnetization space is accumulated. When the histogram becomes “flat,” we reduce the modification factor to a finer one according to the recipe $f_{i+1} = f_i^{1/2}$, reset the histogram $RH(E, M) = 0$, and begin the next random walk. After finishing the initial run we perform 27 cycles, resulting in a final modification factor of 1.000 000 007 45. In our simulations, the flat histogram means that histogram $RH(E, M)$ for all possible (E, M) is not less than 80% of the average histogram. In addition, the histograms are generally checked at each 10 000 Monte Carlo sweeps.

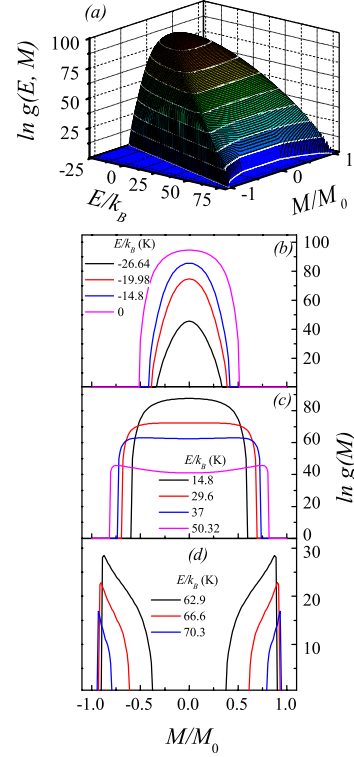


FIG. 1. (Color online) Evaluated DOS $\ln[g(E, M)]$ for $\text{Ca}_3\text{Co}_2\text{O}_6$ compound and curves in (b)–(d) represent the cross-sectioned $\ln[g(E, M)]$ at various energy values E .

After $g(E, M)$ has been obtained, we calculate the thermodynamic and magnetic quantities at any T and B . For example, the internal energy can be calculated by

$$U(T, B) = \frac{\sum_{E, M} H g(E, M) \exp(-H/k_B T)}{\sum_{E, M} g(E, M) \exp(-H/k_B T)} \equiv \langle H \rangle_{T, B}. \quad (3)$$

The magnetization $M(T, B)$ as a function of T and B can be calculated from

$$M(T, B) = \frac{\sum_{E, M} M g(E, M) \exp(-H/k_B T)}{\sum_{E, M} g(E, M) \exp(-H/k_B T)}. \quad (4)$$

Our simulation is performed on $L \times L$ triangular lattices with period-boundary conditions. Unless stated otherwise, $L = 12$ is chosen in this Brief Report. The values of these parameters for the simulation are listed in Table I, and these parameters have been employed for a number of earlier theoretical and simulation works.^{11,14–16}

The simulated DOS $g(E, M)$ for $\text{Ca}_3\text{Co}_2\text{O}_6$ compound is presented in Fig. 1(a). In the low-energy range ($E < 0$), as shown in Fig. 1(b), $g(E, M)$ shows a parabolic shape for a given energy value and reaches its single maximum value at $M = 0$. The calculated DOS at the lowest energy $E_{\min} (\sim -26.64)$ is quite considerable, indicating that the ground state is thus highly degenerate and can be any of a number of spin-frustrated configurations with the same en-

ergy E_{\min} (within the simulation uncertainty). The similar behavior can be observed for some other systems such as $\text{Mo}_{72}\text{Fe}_{30}$.²² In the intermediate energy range ($0 < E/k_B < 62.9$ K), as shown in Fig. 1(c), the single maximum of $g(M)$ at $M=0$ is replaced by a relatively flat profile. It can be observed that the profile becomes wide with increasing E and eventually concave at $E/k_B \sim 37$ K. Furthermore, the possible M range is divided into two separate subranges from $M=0$ when E exceeds 62.9 K. This behavior may stem from the fact that the model has discontinuous degrees of freedom. The two subranges shrink themselves when E further increases, as shown in Fig. 1(d). At the highest energy, only two M states ($M=1, -1$) which correspond to the ferromagnetic orders are possible. Note that the calculated DOS $g(E, M)$ covers all possible (E, M) space, so the thermodynamic and magnetic properties of the system can be accurately evaluated with the former expressions.

The calculated M as a function of T and B is shown in Fig. 2. The magnetization curves clearly show two steps at low temperature ($T < 20$ K). When field B increases from zero, M rapidly reaches the first plateau ($M \sim M_0/3$) and then switches to M_0 above $B \sim 3.6$ T. As it was reported in Ref. 9, the first plateau results from the homogeneous ferrimagnetic order of the spin chains due to the AFM interaction between the chains. As temperature is raised, the steps are progressively washed out due to the thermal activation. When $T > 40$ K, the first step disappears completely and the M - B relation becomes linear. Therefore, our simulation result convincingly demonstrates that the equilibrium state of the perfect triangular lattice of the rigid spins does produce the two-step magnetization curve at low temperature.

It is understood that for realistic materials significant random field as background of the lattice interactions may be available. Now we consider the effect of inhomogeneity in the system. For such a purpose, a random-exchange term $\Delta_{m,n}$ is taken into account. The Hamiltonian can be written as follows:

$$H = \sum_{[m,n]} (J + J\Delta_{m,n}) S_m S_n - B \mu_B g \sum_m S_m, \quad (5)$$

with

$$\Delta_{m,n} = \text{span} \cdot \text{RAM}_{m,n}, \quad (6)$$

where $\text{RAM}_{m,n}$ is the random number in $[-1, 1]$ and span represents the magnitude of the random-exchange term. Such a strategy was extensively accepted for random fields.

In order to compare with earlier work,^{15,16} a random-exchange term with its magnitude $\text{span}=0.15$ is considered first. Figure 3 shows the comparison of the magnetization and internal energy at various T as a function of B for the WL and Metropolis simulations. The two simulations are well coincident with each other at $T=10$ K, as clearly shown in Figs. 3(a) and 3(b), indicating that the Metropolis algorithm also allows the equilibrium state to be reached at relevant T just as the WL method does. However, there is a big discrepancy between the two simulations below $B=3.6$ T at $T=2$ K which is shown in Figs. 3(c) and 3(d). The $M_0/3$ step splits into three equidistant steps in the Metropolis simulation while it keeps invariant in the WL simulation. The relevant internal energies obtained from the Metropolis

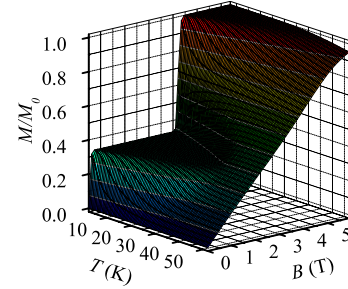


FIG. 2. (Color online) Simulated M/M_0 as a function of T and B .

simulation are higher than the corresponding WL simulation results, as clearly shown in Fig. 3(d), allowing us to argue that the four-step $M(B)$ curve must attribute to the nonequilibrium states. The equilibrium state of the rigid spins can only produce the two-step magnetization curve at $T=2$ K even when the random-exchange term is considered.

Now we can check the dependence of the steplike magnetization feature on the inhomogeneity (random-exchange term) probably available in realistic systems, and the simulated results are presented in Fig. 4(a), where M as a function of B at $T=2$ K upon various span values are plotted in order to understand the effect of the random exchange. One can find that the random-exchange term only smoothens the jumps but cannot assist in generating additional steps. The smoothness of the $M(B)$ curves may be due to the inhomogeneous states induced by the random exchange. As span arises from 0 to 0.3, the borders between the steps become more and more faint. A similar result can also be found in earlier work in which a mean-field approach is employed to study the magnetic properties of the triangular lattice.¹⁶

At last, we come to check the finite-lattice-size effect in our simulations in order to exclude the artificial facts due to the finite lattice size. The simulated $M(B)$ for different L at $T=2$ K upon $\text{span}=0.15$ are plotted in Fig. 4(b). It is demonstrated that the finite-size effect on the magnetization of the system is nearly negligible and our conclusion is reliable.

Our calculated results can be qualitatively explained by means of the spin-configuration analysis. In such a magnetic

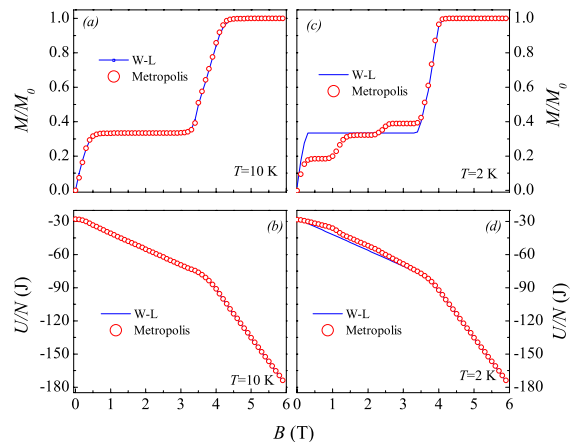


FIG. 3. (Color online) Comparison of (a),(c) M/M_0 and (b),(d) U/N as a function of B calculated from WL method with computed using the Metropolis algorithm at $T=10$ K and $T=2$ K.

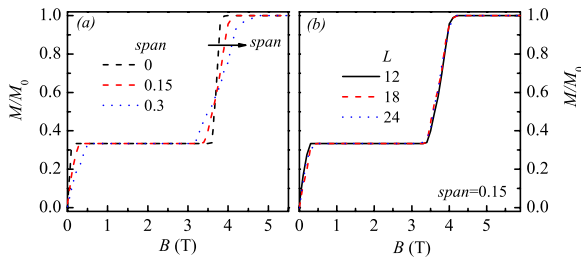


FIG. 4. (Color online) Simulated curves of M/M_0 as a function of B (a) for different spans and (b) for various lattice sizes L at $T = 2$ K.

system, M is determined by the competition between the exchange interaction and applied magnetic field. When the random-exchange term is ignored, antiferromagnetic configurations, $\uparrow\uparrow\downarrow$ (spin-up, spin-up, and spin-down) and $\uparrow\downarrow\downarrow$ appear with the same probability for a triangular sublattice at $B=0$, leading to the zero M . However, a weak B breaks the infinite degeneracy, leaving the ground state $\uparrow\uparrow\downarrow$ corresponding to $M=M_0/3$.³⁰ Such a regular ferrimagnetic structure is formed by taking one spin-down surrounding with six chains of spin-up.¹⁵ As the static magnetic energy increases to be comparable with the interaction energy, the central down spin may flip. The critical field can be estimated to be $6JS/(g\mu_B) \approx 3.6$ T. So when $B > 3.6$ T, the ferromagnetic state $\uparrow\uparrow\uparrow$ is formed. When the random-exchange term is considered, the perfect $\uparrow\uparrow\downarrow$ state may be partially destroyed near the critical fields ($B=0$ and 3.6 T), leading to the smoothness of the $M(B)$ curve.

The present work seems to reveal once more that geometrically frustrated spin systems such as the spin-chain $\text{Ca}_3\text{Co}_2\text{O}_6$ offer very complicated spin configuration which is very sensitive to external fluctuations. Although this argument has been made repeatedly, a reliable experimental approach of the fascinating magnetic phenomena in these frustrated systems becomes extremely challenging in terms of understanding their ground state or equilibrium states. The magnetic property of $\text{Ca}_3\text{Co}_2\text{O}_6$, as an example, has attracted attention for many years, but clear knowledge of its equilibrium magnetization remained ambiguous before the present WL simulation.

In conclusion, we have calculated the magnetization of triangular spin-chain system as a function of temperature and applied magnetic field using the WL method. Our simulation demonstrates that the equilibrium state of the rigid spins produces the two-step magnetization curve at low temperature regardless of the random-exchange term being taken into account or not. The random-exchange term only smoothens the jumps but cannot result in additional steps. It is indicated that the four-step magnetization curve observed in experiments must be due to the nonequilibrium magnetization.

This work was supported by the Natural Science Foundation of China under Grants No. 50832002 and No. 10874075, the National Key Projects for Basic Researches of China under Grants No. 2006CB921802 and No. 2009CB623303, and the 111 Project of the MOE of China under Grant No. B07026.

*liujm@nju.edu.cn

- ¹H. Fjellvag, E. Gulbrandsen, S. Aasland, A. Olsen, and B. Hauback, *J. Solid State Chem.* **124**, 190 (1996).
- ²S. Aasland, H. Fjellvag, and B. Hauback, *Solid State Commun.* **101**, 187 (1997).
- ³H. Kageyama, K. Yoshimura, K. Kosuge, H. Mitamura, and T. Goto, *J. Phys. Soc. Jpn.* **66**, 1607 (1997).
- ⁴H. Kageyama, K. Yoshimura, K. Kosuge, M. Azuma, M. Takano, H. Mitamura, and T. Goto, *J. Phys. Soc. Jpn.* **66**, 3996 (1997).
- ⁵A. Maignan, C. Michel, A. C. Masset, C. Martin, and B. Raveau, *Eur. Phys. J. B* **15**, 657 (2000).
- ⁶V. Hardy, D. Flahaut, M. R. Lees, and O. A. Petrenko, *Phys. Rev. B* **70**, 214439 (2004).
- ⁷V. Hardy, M. R. Lees, O. A. Petrenko, D. McK. Paul, D. Flahaut, S. Hebert, and A. Maignan, *Phys. Rev. B* **70**, 064424 (2004).
- ⁸A. Maignan, B. Hardy, S. Hebert, M. Drillon, M. R. Lees, O. Petrenko, D. M. K. Paul, and D. Khomskii, *J. Mater. Chem.* **14**, 1231 (2004).
- ⁹Y. B. Kudasov, *Phys. Rev. Lett.* **96**, 027212 (2006).
- ¹⁰Y. B. Kudasov, *Europhys. Lett.* **78**, 57005 (2007).
- ¹¹Y. B. Kudasov, A. S. Korshunov, V. N. Pavlov, and D. A. Maslov, *Phys. Rev. B* **78**, 132407 (2008).
- ¹²S. Agrestini, C. Mazzoli, A. Bombardi, and M. R. Lees, *Phys. Rev. B* **77**, 140403(R) (2008).
- ¹³S. Agrestini, L. C. Chapon, A. Daoud-Aladine, J. Schefer, A. Gukasov, C. Mazzoli, M. R. Lees, and O. A. Petrenko, *Phys. Rev. Lett.* **101**, 097207 (2008).
- ¹⁴R. Soto, G. Martinez, M. N. Baibich, J. M. Florez, and P. Vargas, arXiv:0811.4772, *Phys. Rev. B* (to be published).

- ¹⁵X. Y. Yao, S. Dong, and J.-M. Liu, *Phys. Rev. B* **73**, 212415 (2006).
- ¹⁶X. Y. Yao, S. Dong, H. Yu, and J.-M. Liu, *Phys. Rev. B* **74**, 134421 (2006).
- ¹⁷P. L. Li, X. Y. Yao, F. Gao, C. Zhao, K. B. Yin, Y. Y. Weng, J.-M. Liu, and Z. F. Ren, *Appl. Phys. Lett.* **91**, 042505 (2007).
- ¹⁸F. Wang and D. P. Landau, *Phys. Rev. Lett.* **86**, 2050 (2001).
- ¹⁹F. Wang and D. P. Landau, *Phys. Rev. E* **64**, 056101 (2001).
- ²⁰C. Zhou, T. C. Schulthess, S. Torbrügge, and D. P. Landau, *Phys. Rev. Lett.* **96**, 120201 (2006).
- ²¹C. Zhou, T. C. Schulthess, and D. P. Landau, *J. Appl. Phys.* **99**, 08H906 (2006).
- ²²S. Torbrügge and J. Schnack, *Phys. Rev. B* **75**, 054403 (2007).
- ²³M. Troyer, S. Wessel, and F. Alet, *Phys. Rev. Lett.* **90**, 120201 (2003).
- ²⁴W. Koller, A. Prull, H. G. Evertz, and W. von der Linden, *Phys. Rev. B* **67**, 104432 (2003).
- ²⁵Q. Yan and J. J. de Pablo, *Phys. Rev. Lett.* **90**, 035701 (2003).
- ²⁶E. A. Mastny and J. J. de Pablo, *J. Chem. Phys.* **122**, 124109 (2005).
- ²⁷N. Rathore, T. A. Knotts IV, and J. J. de Pablo, *J. Chem. Phys.* **118**, 4285 (2003).
- ²⁸N. Rathore, Q. Yan, and J. J. de Pablo, *J. Chem. Phys.* **120**, 5781 (2004).
- ²⁹G. H. Wannier, *Phys. Rev.* **79**, 357 (1950).
- ³⁰M. Schick, J. S. Walker, and M. Wortis, *Phys. Rev. B* **16**, 2205 (1977).